

# DARPA Y1 (Q1-Q4) Task 3 Report Supplement

## The capillary-astrocyte-neuron (CAN) unit model of energy management in human brain dynamics

### 1. Introduction

As computers, smartphones, and communication networks become more powerful computationally, they also require more power to run. While it is tempting to think that the power consumption of digital devices diminish *pari passu* with smaller integrated circuit (IC) fabrication technology, or even surpass it, this is not the case. For example, even though the process feature size of IC components has been shrinking exponentially over the past several decades in according with Moore's law, the actual microprocessor power consumption has risen at a roughly steady 22% per year (DeMone, 2004; see figure 1):

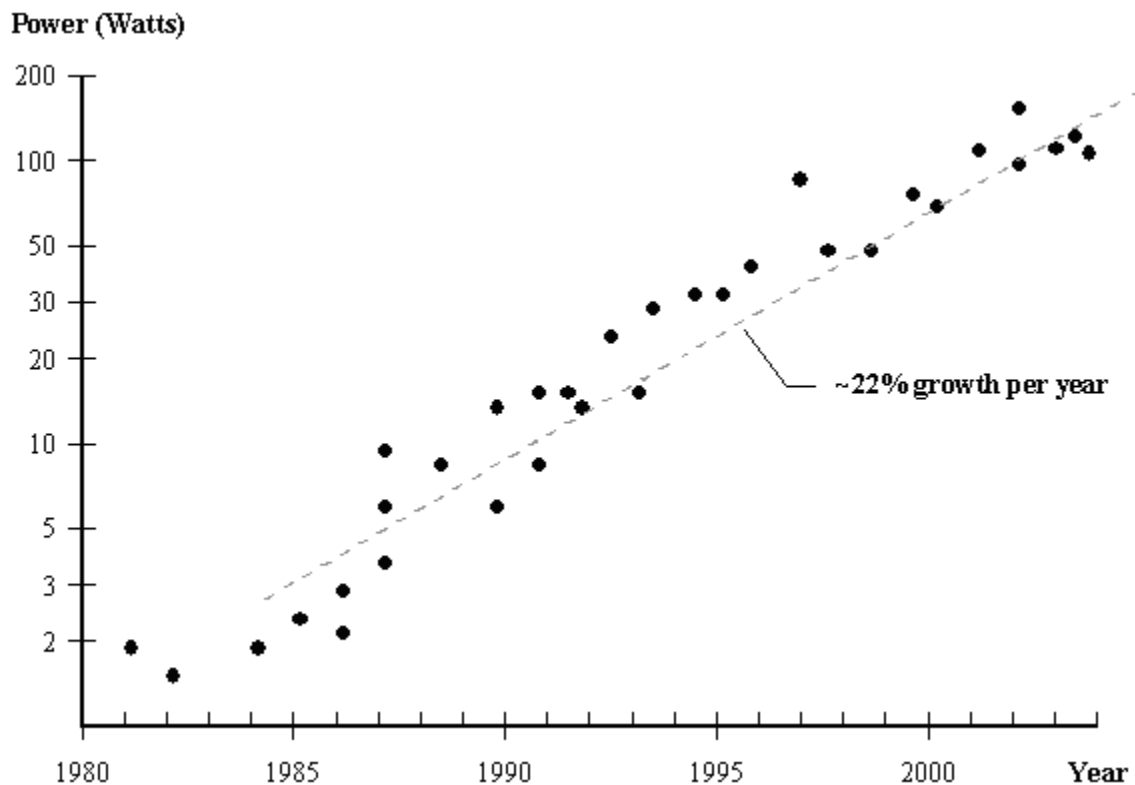


Figure 1: Microprocessor Power Consumption, 1981 to Present. From DeMone (2004)

Attempts by engineers to curtail the energy consumption of digital devices in step with increasing computational power of these devices has had mixed results. Again, as described above, the miniaturization process has been the best friend of the CMOS logic-gate designer as the power consumption per gate reduces precipitously with shrinking process feature size. However, this gift has its limits, as described above. Some other methods that engineers are using to make up the slack include techniques such as “power gating,” which shuts off blocks of the IC that are not currently in use (Roy et al. 2003), and “dual-voltage CPUs,” which vary the voltage between the processor core and input/output operations.

While the above techniques at minimizing the energy consumption in digital devices goes some way toward curbing the rapidly growing energy drain on society that the digital age is forcing us to confront, these techniques will not work when designing future artificially intelligent computational architectures inspired by human brain function. For starters, while miniaturization has worked well in the digital realm, the size of neurons in the mammalian neocortex have remained relatively unchanged for the past 200 million years. While that is not to say that computing architectures designed around the structure of the brain will not benefit from miniaturization, it is notable that this is *not* how the brain developed such massive computational and energy efficiency. Similarly, the brain does not manage its energy consumption through tricks such as power gating or varying its voltage parameters. The reason for this is that, as a massively parallel architecture, it is not possible to cut power to any part of the brain without seriously disrupting the function of the entire organ. In addition, and as we will see later, efficient brain operation depends greatly on managing similar voltage fluctuations across its elements (neurons) in order to produce coherent brain rhythms. Therefore, a “dual voltage” option would not be a useful feature to incorporate into an artificial brain.

In short, while the brain is undeniably a highly computational and energy efficient machine, it manages to accomplish this feat through some mechanism(s) unfamiliar to contemporary electrical and computer engineering practices. As such, it would seem that an investigation into the mechanism the brain does use to manage its computational and energy efficiency would be of interest to the future generation of engineers looking to the biological wisdom of the human brain for guidance. Indeed, in a recent article in the popular electrical-engineering trade journal, *IEEE spectrum*, no fewer than three articles pointed out that, even though the human brain has a computational capacity far outweighing even the largest of today’s supercomputers, it operates at a tiny fraction of the energy consumption of these big computers (Hasler, 2017; Meier, 2017; Rothganger, 2017). Therefore, if we are to address the rapidly growing energy drain on society that the proliferation of computing devices is bringing upon us, it is essential that researchers and engineers soon put forth a serious effort to understand just how it is that human brain efficiency manages its computational and energy efficiency.

Indeed, this is exactly what our team is doing at the Biologically Inspired Neural and Dynamical Systems (BINDS) lab at the University of Massachusetts, Amherst. In our group within the lab, the “Neuro-energetics” group, we have developed a mathematical model/computer simulation

of what we are arguing is the basic metabolic/computational functional unit within the human cerebral cortex. This unit, what we call the “Capillary-Astrocyte-Neuron (CAN)” unit is roughly equivalent in size and structure to the canonical “cortical column” first identified by Mountcastle (1997) as the primary granular or atomistic functional module/unit of cortical operation. In the CAN unit model and its accompanying Matlab computer simulation, we attempt to replicate the complicated cycle of energy flow through the unit by simulating the fluxes of energy precursors and metabolites between the elements of the unit, the electrochemical gradients established across the unit’s constituent neuron, and the integrate-and-fire properties of the neuron in its association with other neurons in the assemblage.

The tentative conclusion we have to after working with the model and its simulation is that the method by which the human brain is able to perform such sophisticated computational feats at such a low energy cost is through 1) coordination of delivery of energy molecule precursors to cooperatively interacting cortical regions, and 2) the phase synchrony in the oscillations of dendritic currents in the CAN unit neuron collectives that populate these interacting cortical regions. More specifically, we argue that the coordinated delivery of nutrients to cooperatively interacting cortical regions set a tempo of the restoral of the resting membrane potential in their constituent neurons which help facilitate the cooperative phase-synchronized, narrow-band oscillations seen between these cooperatively interacting regions.

In order to breakdown the CAN unit model into digestible bites, we will first discuss the justification for the model. Specifically, we will discuss the justification for simplifying the very complicated process of biological-cellular and neurophysiological cortical column dynamics into a few simple equations. Then, we will introduce the “power-grid” metaphor of CAN unit dynamics in order to help facilitate a more user-friendly visualization of the dynamics of the model. After that, we will outline the mathematical equations used in the CAN model as well as some simulation results. Finally, we will discuss what our goals are for future research in the area of neuroenergetics and brain dynamics.

## **2. Justification for “reduced” model**

The typical first step in any effort to model a biological process is to review the available preceding literature/studies on the subject. What we found was that, while there was a good deal of research, *separately*, on the cellular biology of neurons/glia removed from spiking behavior, and research focused on spiking behavior solely, there was essentially no research done on integrating both. Therefore, in initializing this project, we were forced to try to create some sort of manageable hybrid of both the metabolic approach to neurobiology and the more information-processing approach exemplified by the canonical single-neuron “leaky integrate and fire (LIF)” or spiking neuron models that typically eschew any discussion of energy constraints on spiking behavior. The end result of our deliberations on what strategy to use to attack this project was to try to reduce the 50 or so differential equations used to describe the neurobiology of the brain-astrocyte-neuron assemblages in the neocortex reviewed in the Cloutier et al. (2009) model and

merge it with the already simplified Izhikevich (IZ) model (2003) of simple spiking behavior in cortical neurons.

More specifically, we drew inspiration from IZ's approach to reduce the prohibitive number of equations and parameters in the biologically motivated Hodgkin and Huxley model and related models to simulate the spiking behavior of individual neurons and small populations of interacting neurons. In his landmark paper in 2003, IZ published a simplified spiking model of this simple neuron spiking behavior as well as the code to run a simulation of 1000 fully connected neurons. What was especially notable about this effort was that, unlike more simplified LIF neuron models, the reduced IZ formulation boasted the capacity of this simplified model to not only simulate what he referred to as the "regular spiking (RS)" behavior of the typical neocortical neuron, but also the behavior of a collection of other, specialized neurons found in various regions of the telencephalon, such as chattering neurons, intrinsically bursting neurons, low-threshold spiking neurons, and others (IZ).

As far as the metabolic portion of the model inspired by Cloutier et al. (2009), Jolivet et al. (2015) and others, the principal challenge was in deciding which of the biological processes described by the multitude of equations and parameters to include in the CAN model. We decided that the important features of the Cloutier et al. model we wanted to preserve were 1) the flux of glucose from the CBF to astrocyte, 2) the capacity through which the astrocyte can store this glucose energy reserve in form of glycogen (while the neuron cannot), 3) the "astrocyte-neuron lactate shuttle," the mechanism whereby the astrocyte breaks down its glycogen stores to deliver energy in the form of lactate to the neuron in times of need, and 4) the process whereby the neuron metabolizes lactate in the mitochondria to produce ATP, which, in turn, powers the neuron's sodium-potassium pumps.

In short, we were able to reduce the 50 or so equations in the Cloutier et al. (2009) model into two differential equations. The first equation describes the rate of change of the state variable,  $g$ , which is a measure of glycogen/energy store in the astrocyte available for the neuron to utilize. The second equation describes the rate of change of the state variable,  $m$ , which is a measure of the ATP available to reset the membrane potential of CAN unit's representative neuron. From here, we coupled our above formulation, the "reduced Cloutier model," to the canonical IZ model through a parameter in the IZ model related to the resetting of the membrane potential and the  $m$  state variable of the reduced Cloutier model.

While this early form of the CAN model, what we originally called the "reduced IZ-Cloutier" model, showed some interesting behavior in single neuron simulations with a steady metabolic input, it only modeled an open-form flow of energy from the vascular system, through to the astrocyte and neuron, ultimately culminating in its influence on the spiking behavior in the IZ network through the metabolic portion affecting the spiking behavior and frequency of the neuron through its effect on resetting the neuron's membrane potential. In order to close the form of the system of equations, we added a term in the first equation modeling the  $g$  variable

which represented the glutamate concentration in the interstitial matrix surrounding the CAN unit's representative neuron. In experimental studies (Bélanger et al. 2011), this concentration, which is reflective of the metabolic activity of the CAN unit neuron, is sensed by the CAN unit astrocyte and serves to compel that astrocyte to dilate the capillary portion of the CAN unit. Dilating the capillary then serves to deliver more glucose to the astrocyte in response to the increased need for energy precursor molecules demanded via the increased activity in the CAN unit.

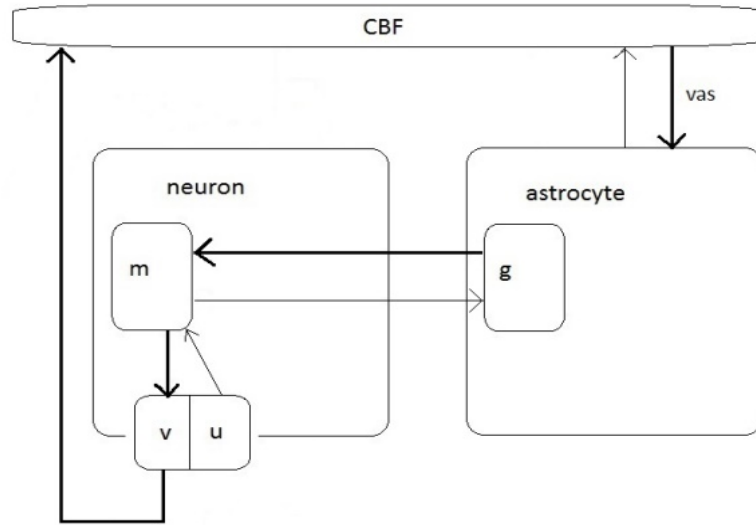


Figure 2: Schematic representation of the CAN unit model showing the flux relations between its various components.

### 3. Power-grid metaphor of CAN unit dynamics

One useful way to visualize how the CAN model views energy management in brain dynamics is by using a power-grid metaphor. Imagine a hypothetical scenario where a small country, Pleasantland, had a half-dozen small power plant stations each driving a power grid for a local community. We'll assign the letters A-E to each of these communities/stations. On the site of each power plant in these communities is a petroleum refinery as well as large storage tanks to hold crude oil to be used in the refinery. The electric generators are driven by the refined petroleum which is refined from the crude oil in the storage tanks as needed on a continuous basis. Once a week, each refinery receives a new shipment of crude oil from a central distribution center deep in the center of the country. The amount of crude that each power station receives each week is determined by the power output of that station the previous week, and that information is given to the crude oil distributors upon delivery of the crude.

In the metaphor above, the electric generators of each power station represent the sodium-potassium-pumps that the CAN unit neuron uses to restore its resting electrochemical membrane potential, the refinery represents the neuron mitochondria that produce ATP to drive those pumps, and the crude oil storage tanks represent the glycogen storage regions of the astrocyte. The weekly distribution routes of the crude oil delivery vehicles represent the human circulatory system/cerebral blood flow, and the central distribution center deep in the center of the country represents the human digestive system which feeds the blood glucose.

To extend this metaphor, let us assume that some of these communities associate with each other in some manner, and some do not. For example, say communities A and C are populated mostly by individuals who share a common religion and who observe strict social practices. Say these practices include daily prayer meetings held in common areas with a television and communications link between the two communities which trigger a spike in the energy demand on the power grid during those times. Now say that communities B and F attract video gamers and that online competition between the two communities in a popular online interactive game is an ongoing event. There are several contests a week and during these events, a large portion of the populace of both communities participate, at which time the energy consumption in each surges simultaneously. Finally, communities D and E share the property of being energy conscious “green” communities whereby a large portion of the houses in each are fully fitted with rooftop solar panels. While communities D and E are connected to and do draw off the country wide electric grid, their energy consumption is attenuated by the offset energy provided by their solar panels. Seeing as the weather in the larger county that houses the six communities is the same, the attenuation of the draw of the main grid in communities D and E is roughly synchronous, although it varies overall week to week.

This extension of the power grid metaphor to include the cooperative behavior within and between the different communities is used to model the formation of resting state networks (RSN) in the human brain. Much in the same way that similar and cooperative activity between the different communities in Pleasantland draw a similar amount of power from the grid in a synchronized fashion, cooperative neocortical regions in the human brain draw a similar amount of energy from the cerebral blood flow and do so in a roughly synchronous fashion. The manner in which these cortical do so is witnessed in the fluctuations in the distribution of blood/nutrients to various regions as witnessed in the Blood-Oxygen Level Dependent (BOLD) signal, which informs the character of fMRI analysis of human brain activity and which serves to identify the various RSN’s that inhabit the human brain.

#### **4. Power-grid metaphor and dynamic synchrony in human brain rhythms**

In the power-grid metaphor, the energy supplied to the individual power stations/communities is a function of the output of electricity that station produces weekly. Similarly, in the CAN unit model, the amount of glucose supplied to the astrocyte is a function of the energy consumed by the associated neurons sodium-potassium pumps. Similarly, in the power-grid metaphor, the

draw on the resources that power the grid rise and fall in relative synchrony in the associated communities, i.e., A-C, B-F, and D-E (see above). Accordingly, during peak times of activity in these associated communities, the draw on crude oil reserves, production from the refinery, and the taxing of the power generators are going to be relatively similar between the communities. This synchrony is important since inconsistencies in the production of power in the grid may lead to inconsistencies in the number and quality of gamers that compete in the periodic online events. These inconsistencies will have significantly negative effect on the quality of the game.

Similarly to the above power-grid scenario, in the CAN unit model, having a similar concentration of ATP in the constitutive neurons or CAN units in cooperatively interacting communities is essential for the requisite synchronous brain rhythms that drive sensory and cognitive processing in those networks. As is revealed in our simulations, the spiking frequency and behavior of neurons is directly affected by the immediate availability or concentration of ATP in the neuron during individual and population spiking “burst” epochs. Therefore, in order to coordinate cooperative activity in these networks, the metabolic cycling of energy precursor molecules must be coordinated between the CAN units that make up the interacting populations.

More specifically, perceptual and cognitive processes in the human brain are accomplished through the formation of what have been referred to as amplitude-modulated (AM) patterns or frames of information in various cortical regions (Freeman, 1991; Kozma and Freeman, 2016; see figures). The AM patterns are formed, as described above, through the cooperative or synchronous activity in a collection of CAN units that compose a cytoarchitecturally circumscribed and defined region of cortex such as the visual cortex (V1) or the motor cortex (M1). Not only are these cognitive perceptual frames coordinated spatially through such synchronization, they are also coordinated temporally as such through a process referred to as chaotic itinerancy. The spatio-temporal coordination of these AM patterns or frames is essential in the formation of perceptions, thoughts, and behaviors in the human nervous system. Disruption of the coordination of these rhythms due to inconsistencies in the energy cycle of the CAN units, such as is witnessed in, say, hypoglycemia or diabetes, lead correspondingly to perceptual-cognitive deficiencies as well as psycho-motor coordination problems (Rosenthal et al., 2001).

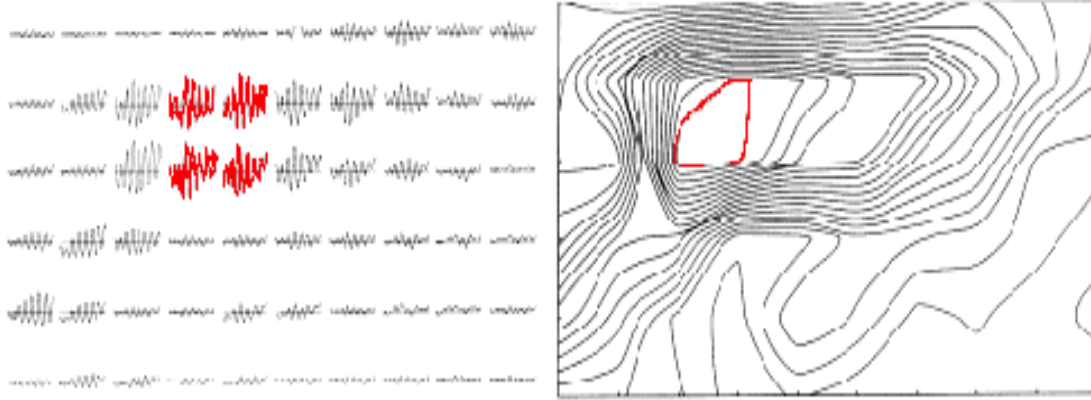


Figure 3: 6x10 micro-array of electrodes implanted on the olfactory cortex of a rabbit (left). Note the commonality of the frequency and phase of each of the 60 EEG recordings on the left. While the frequency and phase of the oscillations are similar across the elements in the array, the amplitudes of each are not. It is these amplitude-modulated (AM) variations across the array that give identity and form to cognitive percepts, and that can be visualized as a topographic map (right). In the current formulation, each of the 60 recordings in the above array can be considered an individual CAN unit coupled into a cooperative network. (image from Freeman, 1991).

## 5. Mathematical model

The mathematical portion of the CAN unit model is composed of four coupled differential equations. Those equations are listed below, followed by a description of the terms and parameters in each equation:

$$\frac{dg}{dt} = \varepsilon\nu \frac{S}{\tau_m} - \frac{\gamma g}{1+m} \quad (1)$$

$$\frac{dm}{dt} = \frac{\gamma g}{1+m} - \mu m \quad (2)$$

$$\frac{dv}{dt} = 0.04v^2 + 5v + 140 - u + I(t) \quad (3)$$

$$\frac{du}{dt} = -0.02u + 0.02v(b + \beta m) \quad (4)$$

In the above-listed set of equations, the first two are a “reduced” representation of the roughly 50 differential equations which comprise the Cloutier et al. metabolic model, while the second two are essentially identical to the canonical IZ model, with the exception of the added “ $\beta m$ ” term in equation (4) that serves as the main state variable that couples the IZ model to the reduced Cloutier et al. model.

Equation (1) represents the glycogen stores in the astrocyte portion of the CAN unit immediately available to the neuron as energy to drive the neurons’ Krebs cycle in the production of ATP there.  $D(g)/dt$  reflects the change in the glycogen concentration in the astrocyte as a function of the glucose delivered there via the cerebral blood flow (CBF), represented by the expression  $\varepsilon v(S/\tau_m)$ , as well as the ratio of available glycogen stores ( $g$ ) in the astrocyte to the current concentration of ATP in the neuron.  $\varepsilon$  and  $\gamma$  are proportionality constants, and  $S$  is a reflection of the level of synaptic activity on the neuron dendrites of the neuron portion of the CAN unit. As the CAN model in its current form is a fully connected network,  $S$  represents the summation of the voltage-potential values of the neuron,  $V$ , across 100 time steps. This average is then divided by 100 ( $\tau_m$ ), to give an average value of the potential over that 100 ms epoch. The significance of the value of  $S$  lies in that it is used here to represent the concentration of the excitatory neurotransmitter glutamate in the synaptic clefts and interstitial matrix of the CAN unit which has been shown to influence the constriction and dilation of the capillary portion-CBF flow of the CAN unit (Bélanger et al. 2011). The last term in the equation,  $(\gamma g/1+m)$ , reflects the ratio of available glycogen stores, ( $g$ ), in the astrocyte to the current concentration of ATP in the neuron. Higher values of ( $g$ ) will attenuate the rate of increase of glycogen stores relative to the contribution by the CBF. Higher values of ( $m$ ) indicate that the neuron is currently flush with ATP and so acts to increase the buildup of glycogen stores ( $g$ ).

Equation (2) represents the ATP availability in the neuron to be used in the restoration or resetting of the membrane potential there. The restoration of the membrane potential consumes the majority of the ATP in the neuron cell and is responsible for the efficiency whereby the neuron performs its critical “integrate and fire” duties. The state variable in this equation is ( $m$ ), and the term  $d(m)/dt$  reflects the change in the concentration of ATP in the neuron available to reset the membrane potential through driving the neuron’s sodium-potassium pump. As in equation (1), the term  $(\gamma g/1+m)$ , reflects the ratio of available glycogen stores in the astrocyte to the current concentration of ATP in the neuron and serves a similar regulatory role as in equation (1). In relation to this equation (2), higher values of  $m$  indicate a relative saturation of ATP in the neuron and, thus, will attenuate the rate of increase in ATP production. Higher values of  $g$  indicate that, should the concentration of ATP ( $m$ ) in the neuron be low, there is a large supply of glycogen (energy) that the neuron can utilize to produce more ATP. Thus, larger ratios of  $g/m$  in this equation will drive a positive rate of change of ATP production. The  $(-\mu*m)$  term reflects the exponential decay of  $m$  as parameterized by the constant  $\mu$ . The exponential decay is modeled as a process whereby ATP is continually consumed by the neuron as a steady function of the demand of the sodium potassium pumps to reset the resting membrane potential. Having

this term present in the equation is also essential for the simulation to produce oscillatory behavior in the metabolic network.

Equation 3 is one half of the canonical IZ simple-spiking neuron model and has been unchanged in the current formulation of the CAN model. The state variable in this equation is  $V$ , and  $d(V)/dt$  reflects the rate of the change of the voltage potential across the CAN unit neuron as a function of the values of the variables  $U$  and  $I(t)$ . The first portion of the equation combine three terms into the expression  $(0.02V^2 + 5V + 140)$  which has been carefully formulated by Izhikevich (2003) to produce biologically realistic firing patterns in individual neurons and small population of neurons. The parameters which affect the specifics of the spiking behavior are found in the two terms that follow it,  $u$  and  $I(t)$ .  $I(t)$  represents the influences of the other neurons' axons in the network impinging on the CAN unit target neuron in question. The influence of  $I(t)$  can be divided into positive and negative effects depending on whether the input is coming from the excitatory neurons or inhibitory neurons of the network. Greater values of  $I(t)$  will drive  $dV/dt$  higher as it reflects a greater contribution of excitatory synaptic activity. The term  $U$  is the state variable of equation (4) and its function is to modulate the value of  $V$  by counteracting the depolarizing effect of high  $I(t)$  values.  $U$  represents the actions of ATP on the neuron's sodium-potassium pump in the effort to restore the resting membrane potential to a value of  $-70$  mV.

Equation 4 is the second half of the canonical IZ simple-spiking neuron model and has been slightly modified in order to couple the IZ spiking-neuron model to the Cloutier portion of the model. What has been added is the  $(\beta * m(t))$  term, which reflects the contribution of the time-varying concentration of ATP stores in the spiking dynamics of the canonical IZ model and simulation. The state variable in this equation is  $U$ , and  $d(U)/dt$  reflects the strength through which the neuron's resting membrane potential is reset or more specifically, is *resistive* to the depolarizing effects of high excitatory neuron  $I(t)$  values in equation (3). Again, the first two terms in the expression  $(-0.02U + 0.02V(b))$  are taken unchanged from the canonical IZ model. The last term,  $(0.02 * V * (\beta) * m(t))$  relates the scaling factor  $(\beta)$  to the current concentration of ATP in the neuron available to do work running the neuron's sodium-potassium pump in the effort to restore the neuron's resting membrane potential.

## 6. Computer simulation

Simulation runs of the CAN-unit model were carried out using MATLAB. Our efforts in this paper focused on finding optimal parameters which produced robust gamma oscillatory behavior in each CAN unit while keeping the values of the energy related ( $m$ ) and ( $g$ ) state variables “well behaved” and normalized between the values of 0 and 1. The reasons we chose these criteria to govern the parameterization of the model is 1) robust gamma oscillations are a defining characteristic of *in vivo* ECoG or local field potential recording in brain cortical columns, and 2) “non-well-behaved” values of ( $m$ ) and ( $g$ ) that stray outside of the normalized range often shift the behavior of the IZ spiking neurons into that of a “chattering mode,” which is more

characteristic of non-cortical neurons rather than the “regular spiking” behavior of cortical-pyramidal neurons.

### 6.1 Range of optimal parameter values

We wanted gamma oscillations among the neurons in such a way that the observed gamma behavior is not the result of chattering behavior (that is often associated with high synchrony among the neurons). Hence, we came up with a new metric (based on Power Spectral Density) that serves as an indicator of the kind of desirable behavior that we were looking for; described here:

An average signal  $V_{avg}(t)$  is calculated by averaging the membrane potential  $V_n(t)$  of all neurons at each time step from  $t$  from 1501 milliseconds to 2500 milliseconds:

$$V_{avg}(t) = \frac{1}{N} \sum_{n=1}^{N_e} V_n(t)$$

$V_{avg}(t)$  is now filtered using a bandpass gamma filter. The filtered signal is then split into successive 25 segments of size 40 milliseconds each. For each segment the standard deviation is obtained and variance among the standard deviation of all such 25 segments is obtained.

The measure obtained is denoted by  $\phi$  and it was computed for all combinations of  $\beta, \varepsilon$  such that  $\beta = 0:0:01:0:2$ ,  $\varepsilon = 0 : 0:01 : 1$ . The plot can be seen below:

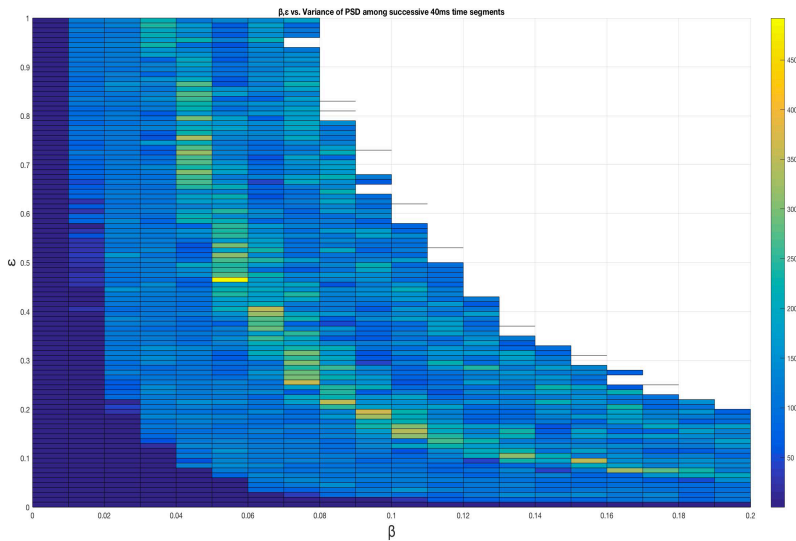


Figure 10: The deep blue regions in the other plot represent low variance of power spectral

density among the 40ms segments. Low variance of power spectral implies less chattering behavior (chattering results in pseudo gamma behavior where the spikes are not uniformly distributed but confined to certain compact intervals). This also implies that there is gamma activity in the cortical column (there are spikes in the cortical column at gamma frequency) but not necessarily at the level of individual neurons. Within the deep blue regions it was also necessary to make sure that values of  $m$  and  $g$  stayed within the range  $[0,1]$ . After thoroughly analyzing the impact of values of  $\beta$  and  $\epsilon$  within the deep blue region (and also a few values outside this range around the fringes), we now have a range of  $\beta$  and  $\epsilon$  values for which the values of  $m$  and  $g$  stay within  $[0,1]$ . The optimal parameter values include:  $\beta=[0\dots0.1]$ , and  $\epsilon=[0\dots0.04]$ .

## 6.2 Study of 'good' parameter space

A number of experiments were carried on to assess the impact of the range of optimal parameter values on power and amplitude synchrony of the excitatory neurons in the gamma, theta band as well as the unfiltered signals.

### 6.2.1 Power in the gamma band

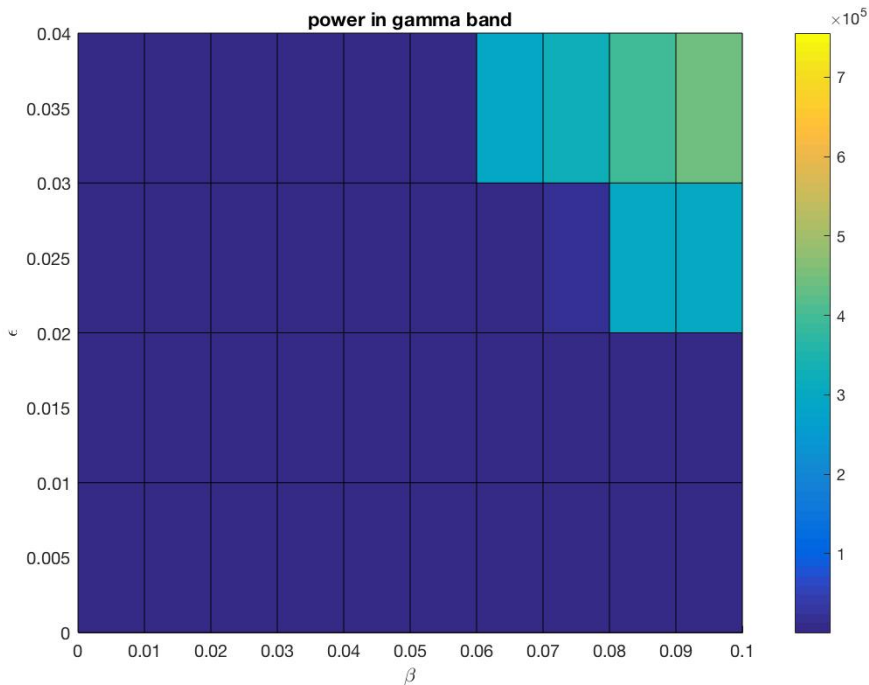


Figure 11: The plot shows the power in gamma band vs. parameters  $\beta$  and  $\epsilon$ . The mean of the original spike train at every time step was obtained. This 'average' signal was filtered so that only elements in the gamma band were retained (40Hz-60Hz). For this filtered average signal, the power was computed by squaring the magnitude of the signal at each time step and then summing it up.

## 6.2.2 Power in Theta band

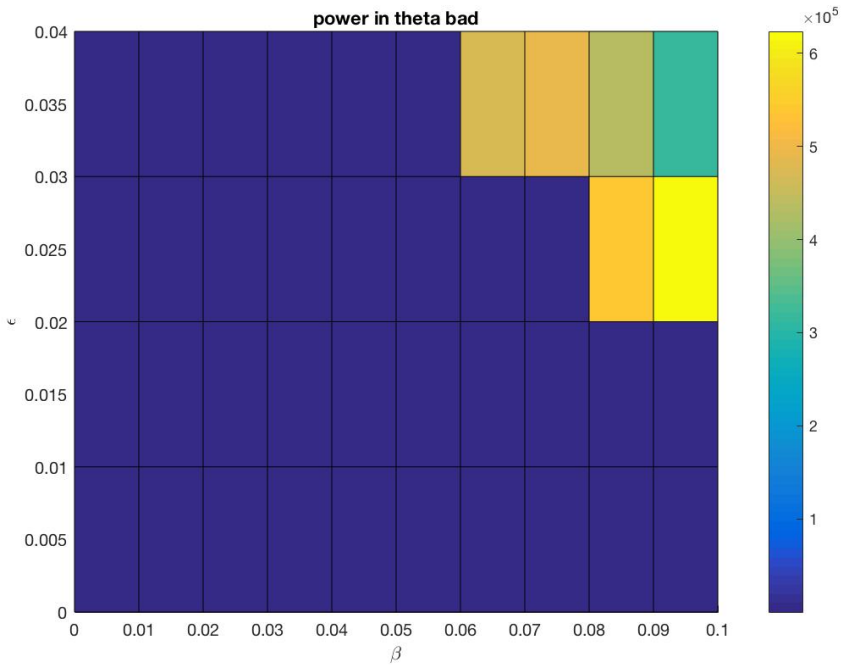


Figure 12: The plot shows the power in theta band. The mean of the original excitatory spike trains at every time step was obtained. This 'average' signal was filtered so that only elements in the theta band were retained (4Hz-7Hz).

## 6.2.3 Power in unfiltered signal

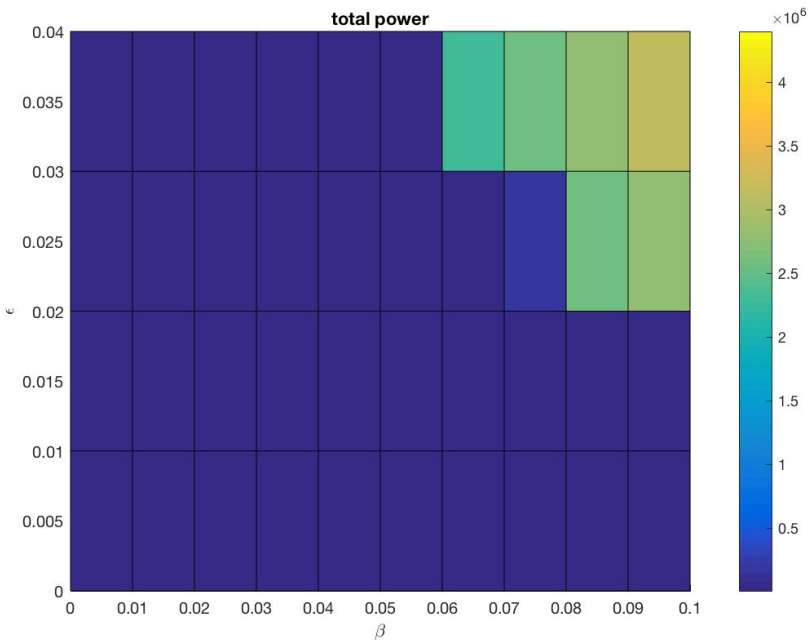


Figure 13: The plot shows the total power in the average excitatory signal vs. parameters  $\beta$  and  $\epsilon$ . The mean of the original spike trains of the excitatory neurons at every time step was obtained. For this 'average' signal, the power consumed between 1501 milliseconds to 2500 milliseconds was computed by squaring the magnitude of the signal at each of those time step and then summing it.

### 6.2.4 Amplitude Synchrony in unfiltered signal

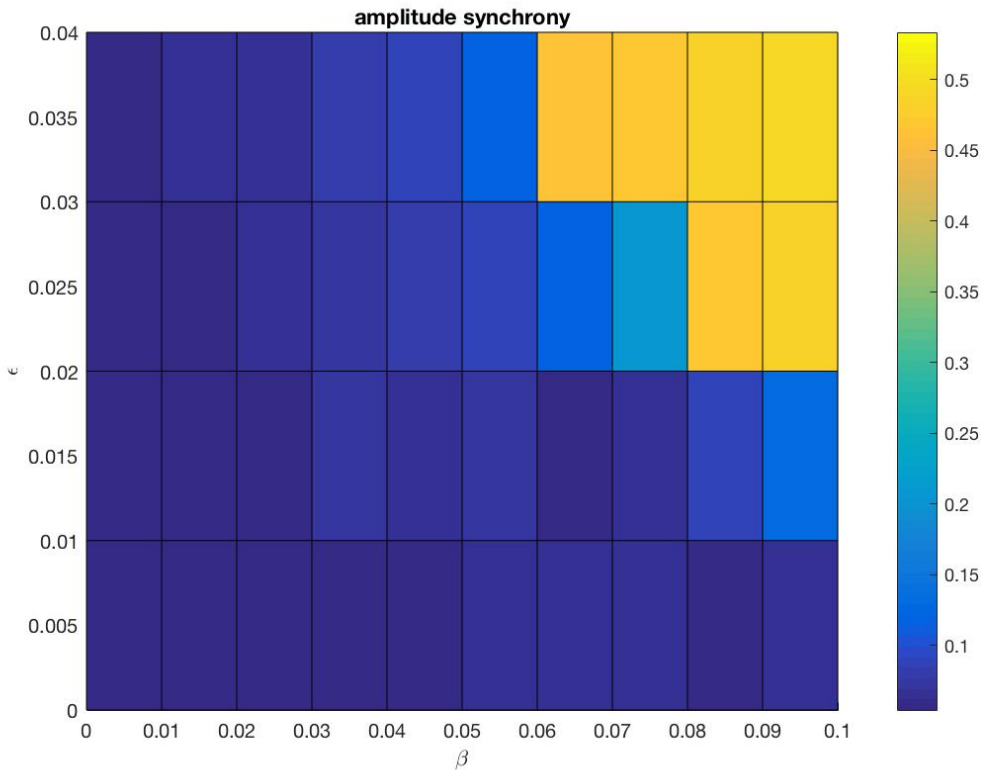


Figure 14: The plot shows the amplitude synchrony among the unfiltered signals vs. parameters  $\beta$  and  $\epsilon$ . The amplitude synchrony between 1501 to 2500 milliseconds was computed by considering all the original unfiltered signals of the individual neurons

## 6.2.5 Raster array

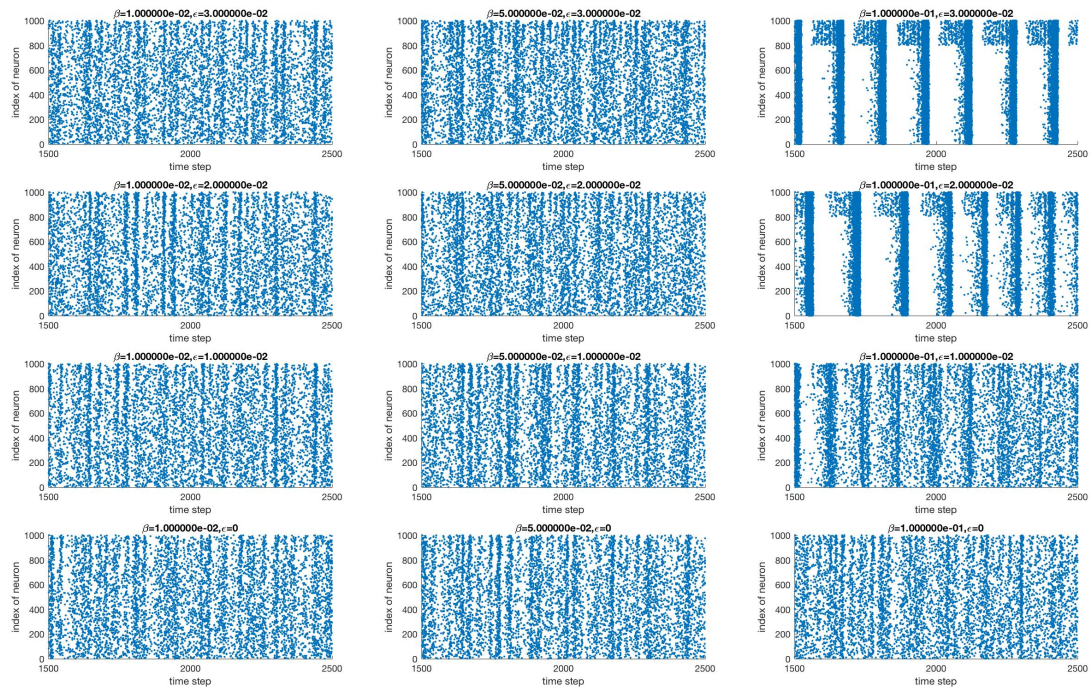


Figure 15: Raster plots depicting the change in amplitude synchrony across an array of optimized parameter values.

## 7. CAN model interactive interface

Since resetting the model parameters within the Matlab code every time we wanted to test a new combination of parameters was time consuming and tedious, we have recently developed an interactive GUI interface whereby the parameters can be changed much more conveniently and the results witnessed in real time. This interface is available on the BINDS website:

<https://binds.cs.umass.edu/neuroEnergeticsMain.html>

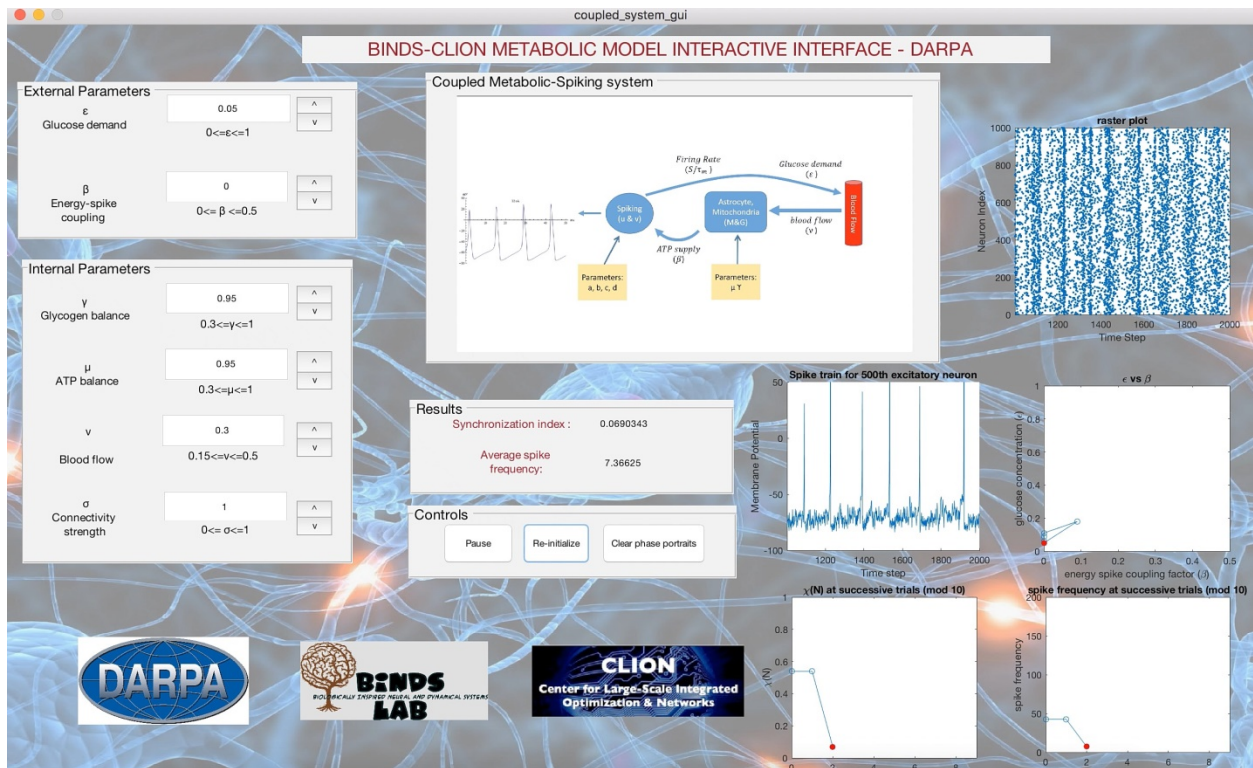


Figure 16: CAN model interactive interface.

## 8. Conclusion and future directions

The main conclusion to be drawn from the research done in developing the CAN unit model is that the human brain manages its energy stores through 1) coordinating the distribution of energy precursors to cooperatively interacting cortical regions and 2) utilizing the coordinated energy cycles of those cooperating regions to aid in the synchronization of activity between those regions. Coordinating the timing of the dynamics rhythms of dendritic currents allow for an energy efficient means for constructive interference in those networks to sharpen the identity of cognitive-perceptual AM patterns in cortical neuropil with minimal wasted energy being dissipated due to excessive phase dispersion and frequency modulation in the network. While it is unclear whether the lessons learned here will be of any benefit in designing the next generation of traditional, serial-based integrated circuit technology, it will certainly be of great benefit when designing the next generation of massively parallel computing architectures inspired by the computationally impressive and energy efficient human brain.

## References:

Bélanger M, Allaman I, Magistretti PJ. (2011). Brain energy metabolism: focus on astrocyte-neuron metabolic cooperation. *Cell Metabolism* 14(6):724-38

Cloutier, M., Bolger, F.B., Lowry, J.P. and Wellstead, P. (2009). An integrative dynamic model of brain energy metabolism using in vivo neurochemical measurements. *Journal of Computational Neuroscience*, 27(3), pp.391-414.

DeMone, P. (2004) "The Incredible Shrinking CPU: Peril of Proliferating Power".

<http://www.realworldtech.com/shrinking-cpu/3/>

Freeman, W. J. (1991) The physiology of perception. *Scientific American*, 264(2):78-85

Hasler, J. (2017) A road map for the artificial brain. *IEEE spectrum* (6-17), pp. 47-50.

Hodgkin, A.L. & Huxley, A.F. (1952). A quantitative description of membrane current and its application to conduction and excitation in nerves. *J. Physiol. (London)* 117, 500-544.

Izhikevich, E.M., 2003. Simple Model of Spiking Neurons. *IEEE Transactions on Neural Networks*, 14(6), pp.1569-1572.

Jolivet, R., Coggan, J.S., Allaman, I., Magistretti, P.J., (2015). Multi-timescale modeling of activity-dependent metabolic coupling in the neuron-glia vasculature ensemble. *PLoS Computational Biology*, 11(2), e1004036.

Kozma, R. and Freeman, W.J., 2016. "Cognitive phase transitions in the cerebral cortex-enhancing the neuron doctrine my modeling neural fields." Springer. New York.

Meier, K. (2017) The brain as computer. *IEEE spectrum* (6-17), pp. 29-33.

Mountcastle V. B. (1997) The columnar organization of the neocortex. *Brain* 120, pp. 701–22.

Nelson, M.E. (2004) *Electrophysiological Models In: Databasing the Brain: From Data to Knowledge.* (S. Koslow and S. Subramaniam, eds.) Wiley, New York.

Rosenthal JM, Amiel SA, Yágüez L, Bullmore E, Hopkins D, Evans M, Pernet A, Reid H, Giampietro V, Andrew CM, Suckling J, Simmons A, Williams SC. (2001).

The effect of acute hypoglycemia on brain function and activation: a functional magnetic resonance imaging study. *Diabetes* 50(7):1618-26.

Rothganger, F. (2017) The dawn of the real thinking machine. *IEEE spectrum* (6-17), pp. 23-25.

Roy, K. et. al. (2003) "Leakage current mechanisms and leakage reduction techniques in deep-submicrometer CMOS circuits", *Proceedings of the IEEE*